

# Quasi-Classical Trajectory Study of the F + CD<sub>4</sub> Reaction Dynamics

Joaquín Espinosa-García<sup>†</sup>

Departamento de Química Física, Universidad de Extremadura, 06071 Badajoz, Spain

Received: January 30, 2007; In Final Form: March 9, 2007

To analyze the F + CD<sub>4</sub> gas-phase abstraction reaction, an exhaustive state-to-state dynamics study was performed. Quasi-classical trajectory (QCT) calculations, including corrections to avoid zero-point energy leakage along the trajectories, were used on an analytical potential energy surface (PES-2006) recently developed by our group for collision energies in the range 0.3–6.0 kcal mol<sup>-1</sup>. While the CD<sub>3</sub> coproduct appears vibrationally and rotationally cold, in agreement with experiment, most of the available energy appears as FD( $\nu'$ ) product vibrational energy, peaking at  $\nu' = 3$ , one unit colder than experiment. The excitation function reproduces experiment, with the maximum contribution from the most populated FD( $\nu' = 3$ ) level. The state-specific scattering distributions at different collision energies also reproduce the experimental behavior, with a clear propensity toward forward scattering, this tendency increasing with the energy. These dynamics results show the capacity of the PES-2006 surface to correctly describe the title reaction.

## I. Introduction

The hydrogen abstraction reaction of fluorine atoms with methane and its isotope analogues has received much attention, both theoretical and experimental, in recent years. This reaction is very exothermic, very fast, and presents a very low barrier height.

In a very recent work,<sup>1</sup> we constructed a new analytical potential energy surface (PES) for the F + CH<sub>4</sub> → FH( $\nu',j'$ ) + CH<sub>3</sub>( $\nu,j$ ) reaction and its isotope analogues. This surface, named PES-2006, remarkably improved the kinetics and dynamics results of earlier surfaces of our group, PES-1996<sup>2</sup> and PES-2005.<sup>3</sup> The main differences with respect to the earlier surfaces<sup>2,3</sup> lie in the calibration process. The criterion chosen for the PES-2006 was broader than in previous works of our group.<sup>2,3</sup> As usual, we tried to reproduce the experimental variation of the forward rate constants with temperature in the experimentally measured range (180–410 K). However, the main innovation with respect to earlier surfaces is that we tried also to reproduce the topology of the reaction, from reactants to products, with especial care taken in the reproduction of ab initio information along the reaction path and the investigation of complexes in the entry and exit channels. Therefore, in that paper<sup>1</sup> we did not limit the calibration to the zone close to the saddle point. On this surface, we studied exhaustively the kinetics, using variational transition-state theory (VTST) with semiclassical transmission coefficients, as well as the dynamics using quasi-classical trajectory (QCT) calculations including corrections to avoid zero-point energy leakage along the trajectories. We concluded that the reasonable agreement with experiment (always qualitative and sometimes quantitative) lends confidence to the new PES-2006 surface.

To go deeper into the understanding of this reaction and the role of the isotopic substitution, in the present paper we perform a QCT dynamics study of the F + CD<sub>4</sub> → FD( $\nu',j'$ ) + CD<sub>3</sub>( $\nu,j$ ) reaction using the analytical PES-2006 surface. In a series of recent experimental works, Liu and co-workers<sup>4–7</sup> studied this reaction exhaustively using the time-sliced ion velocity imaging

technique to obtain the state-specific correlation of co-incident product pairs. They analyzed the integral cross section, its variation with the collision energy (i.e., the excitation function), and the product scattering angular distribution (measured as the differential cross section, DCS). They concluded that this reaction is direct and its dynamics properties differ from those for the analogue F + CH<sub>4</sub> reaction. These very interesting experimental data can be used to test the accuracy of the recently developed PES-2006 surface.

The article is structured as follows. In section II, we briefly outline the potential energy surface and the computational details in the QCT calculations. The dynamics results are presented in section III, and for different dynamics properties, are compared with those for the analogue F + CH<sub>4</sub> reaction. Finally, section IV presents the conclusions.

## II. Potential Energy Surface and Computational Details

Recently, our group constructed a new PES for the gas-phase F + CH<sub>4</sub> → FH + CH<sub>3</sub> polyatomic reaction,<sup>1</sup> PES-2006, which is symmetric with respect to the permutation of the methane hydrogen atoms, a feature especially interesting for dynamics calculations. The functional form was developed in that work and therefore will not be repeated here. Basically, it consists of four London–Eyring–Polanyi (LEP) stretching terms, augmented by out-of-plane bending and valence bending terms. In the calibration process, we fitted some of the parameters of the analytical PES to reproduce the variation of the experimental thermal forward rate constants with temperature (as in earlier papers of our group) and the topology of the reaction from reactants to product with special care taken in the reproduction of ab initio information along the reaction path and the investigation of complexes in the entry and exit channels, which was an innovation with respect to earlier papers.

The title reaction consists of a hydrogen abstraction reaction from perdeuterated methane to yield the perdeuterated methyl radical, with a slow change in the geometry of the methyl group from pyramidal to planar along the reaction path. The reactant and product properties (energy, geometry, and vibrational frequency) are listed in Table 1 and are compared with

<sup>†</sup>E-mail: joaquin@unex.es.

**TABLE 1: Reactant and Product Properties<sup>a</sup> Calculated Using the Analytical Surface**

	CD <sub>4</sub>		CD <sub>3</sub>		FD	
	PES-2 006	expt <sup>b</sup>	PES-2 006	expt <sup>c</sup>	PES-2 006	expt <sup>d</sup>
$R_{C-D}$	1.094		geometry			
angle 1 <sup>e</sup>	109.5		1.094			
angle 2 <sup>f</sup>	120.0		120.0			
$R_{F-D}$			180.0		0.917	0.919 <sup>g</sup>
			frequency			
	2311	2259	2368	2381	2983	2998
	2311	2259	2368	2381		
	2311	2259	2173	2158		
	2111	2109	1017	1026		
	1088	1092	1017	1026		
	1088	1092	450	458		
	1024	996				
	1024	996				
	1024	996				
			energy			
$\Delta H_r^h$	-30.95					
ZPE	20.43	20.10	13.43	13.48	4.26	4.28

<sup>a</sup> Distances in Å, frequencies in cm<sup>-1</sup>, energies in kcal mol<sup>-1</sup>. <sup>b</sup> Experimental data from ref 8a. <sup>c</sup> Experimental data from ref 8b. <sup>d</sup> Experimental data from ref 8c. <sup>e</sup> Angle 1: Bond angle D-C-D, in degrees. <sup>f</sup> Angle 2: Dihedral angle in degrees. <sup>g</sup> Experimental value from ref 8d. <sup>h</sup> Enthalpy of reaction at 0 K.

experiment. In general, the reactant and product properties agree very well with the experimental vibrational frequencies.<sup>8</sup>

Because of the abundant experimental information available for this reaction, PES-2006 was subjected to a great variety of tests, both kinetics and dynamics. Thus, from the kinetics point of view, first, the forward thermal rate constants calculated using variational transition-state theory (VTST) with semiclassical transmission coefficients agreed with experimental measurements, reproducing the Arrhenius plot. Second, we found good agreement at several temperatures of the CH<sub>4</sub>/CD<sub>4</sub> kinetic isotope effects (KIEs), which are a very sensitive test of features of the new surface, such as barrier height and width, zero-point energy, and tunneling effect.

From the dynamics point of view, an extensive study employing quasi-classical trajectory (QCT) calculations was also performed on this surface. First, we found that the FH( $\nu'$ ,  $j'$ ) rovibrational distributions agree with experiment. Second, the state-specific scattering distributions present qualitative agreement with experiment, and as the FH( $\nu'$ ) vibrational state increases the scattering angle becomes more forward. Third, the oscillatory pattern in the excitation function, the forward/backward predominance in the differential cross section (DCS) analysis, and the dramatic change in the three-dimensional "DCS-collision energy-scattering angle" plot are signatures of the resonance reported experimentally by Shiu et al.<sup>9</sup> and are assigned to quasi-bound states in the vibrationally adiabatic curve as found in our surface. Obviously, the classical nature of the QCT calculations means that this conclusion is only tentative, and quantum-mechanical (QM) calculations will be required for a firmer conclusion to be drawn. In sum, this reasonable agreement lends confidence to this PES-2006 polyatomic surface, although there are some differences which, of course, may be due to the PES itself but also to the known limitations of the QCT method (especially the binning procedure).

Quasi-classical trajectory (QCT) calculations<sup>10-12</sup> were carried out using the VENUS96 code,<sup>13</sup> customized to incorporate our analytical PES. Moreover, a modification was included to compute the vibrational energy in each normal mode to obtain information on the CD<sub>3</sub> coproduct vibrational distribution in

**TABLE 2: Product Energy Partition at a Collision Energy of 5.4 kcal mol<sup>-1</sup>**

	PES-2006	expt <sup>a</sup>	PES-2005 <sup>b</sup>	CABMFV <sup>c</sup>
$f_v(\text{FD})$	0.69		0.32	0.52
$f_R(\text{FD})$	0.06		0.22	0.05
$f_v(\text{CD}_3)$	0.09	0.05	0.26	0.21
$f_R(\text{CD}_3)$	0.04	0.02	0.02	0.02
$f_T$	0.12		0.19	0.20

<sup>a</sup> Reference 5. <sup>b</sup> LEPS-type PES from ref 3. <sup>c</sup> Interpolated ab initio PES at the MP-SAC2 level from ref 25.

the exit channel. Since VENUS freely rotates the molecules along the trajectories, the normal-mode energy calculation is preceded by a rotation of the molecule to maintain the orientation of the optimized geometry of the methane molecule for which the normal-mode analysis was performed. Once this is done, a projection of the displacement and momentum matrices on the normal-mode space allows one to compute the potential and kinetic energy for each normal mode. The energy in each harmonic normal mode was computed for the last geometry (coordinates and momenta) on the reactive trajectories. Since the harmonic approximation was used for this calculation, one could expect a breakdown of the procedure for highly excited states. However, as we are interested in the CD<sub>3</sub> vibrational ground state, we can assume that this method is accurate enough for the present purpose. This approach had been used in earlier papers by our group<sup>1,14</sup> with excellent results.

The accuracy of the trajectory was checked by the conservation of total energy and total angular momentum. The integration step was 0.01 fs, with an initial separation between the F atom and the perdeuterated methane center of mass of 6.0 Å, a maximum value of the impact parameter of 3.5 Å, and a methane rotational energy of 20 K. The reagent collision energies considered in the present work range from 0.3 to 6.0 kcal mol<sup>-1</sup>, and batches of 50,000 trajectories were calculated at each energy, where the impact parameter,  $b$ , was sampled by  $b = b_{\text{max}} R^{1/2}$ , with  $R$  being a random number in the interval [0,1].

A serious drawback of the QCT calculations is related to the question of how to handle the quantum mechanical zero-point energy (ZPE) problem in the classical mechanics simulation.<sup>15-24</sup> Many strategies have been proposed to correct for this quantum-dynamics effect (see, for instance, refs 15-19 and 22 and references therein), but no completely satisfactory alternatives have emerged. Here, we employed a pragmatic solution, the so-called passive method,<sup>19</sup> consisting of discarding all the reactive trajectories that lead to either an FD or a CD<sub>3</sub> product with a vibrational energy below their respective ZPE. This we call histogram binning with double ZPE correction (HB-DZPE).

### III. Results and Discussion

**(A) Product Energy Partition.** The QCT results on the PES-2006 at a collision energy of 5.4 kcal mol<sup>-1</sup> are listed in Table 2 together with the sparse experimental data<sup>5,6</sup> and other QCT results on different surfaces.<sup>3,25</sup> It was found experimentally that the CD<sub>3</sub> coproduct appears with a moderate amount of internal energy, 6-8% of the total available energy. The PES-2006 results qualitatively agree with experiment and notably improve the results from previous surfaces, interpolated ab initio,<sup>25</sup> and our earlier PES-2005.<sup>3</sup>

To perform a deeper comparison with experiment,<sup>6</sup> Table 3 lists the energy disposal into FD product and relative translation for the CD<sub>3</sub>( $\nu = 0$ ) coproduct, that is, in its vibrational ground state, at several collision energies. Taking into account that the experiment only provides the relative reaction cross section, the

**TABLE 3: Reaction Cross Section,  $\sigma(\text{\AA}^2)$ , and Energy Disposal into  $\text{FD}(\nu', j') + \text{CD}_3(\nu = 0)$  Products, in  $\text{kcal mol}^{-1}$** 

$E_{\text{coll}}^a$	1.5	2.75	5.4
$\sigma_{\text{rel}}^b$	0.41	0.85	1.21
	0.67	0.93	1.31
$\langle E_{\nu'} \rangle_{\text{FD}}$	30.7	30.0	28.8
	29.0	29.4	30.0
$\langle E_{\text{R}} \rangle_{\text{FD}}$	0.12	0.67	1.1
	1.40	1.69	2.13
$\langle E_{\text{T}} \rangle$	1.3	3.0	6.3
	2.5	3.6	4.8

<sup>a</sup> Experimental collision energies are, respectively: 1.48, 2.77, and 5.37  $\text{kcal mol}^{-1}$ , ref 6. <sup>b</sup> The first entry corresponds to experiment and the second to QCT.

PES-2006 results reproduce the experimental behavior. This surface finds first that most of the reaction energy is deposited into the vibration of the FD product, in agreement with experiment, second, that the energy deposited into FD rotation is greater than experiment, and therefore a greater FD rotational distribution will be expected than experiment, and third, that the relative translational energy increases with the collision energy, which agrees with the experimentally observed propensity  $T(\text{or } E_{\text{coll}}) \rightarrow T'$  in this reaction.

**(B) Excitation Function.** The QCT total excitation function (reaction cross section versus collision energy) and the  $\text{FD}(\nu')$  components are plotted in Figure 1 for the  $\text{CD}_3(\nu = 0)$  coproduct, that is, in its vibrational ground state, for direct comparison with experiment.<sup>5</sup>

Zhou et al.<sup>5</sup> found experimentally that the threshold of the reaction is  $\approx 0.5 \text{ kcal mol}^{-1}$  and that the total reaction cross section rises rapidly from the threshold and then levels off at higher collision energies. The PES-2006 reproduces this experimental behavior with a reaction barrier of  $0.35 \text{ kcal mol}^{-1}$ . In considering the  $\text{FD}(\nu')$  vibrational state contribution to this function, we found that the most populated  $\text{FD}(\nu' = 3)$  state follows the same tendency, the  $\text{FD}(\nu' = 2)$  state shows a practically isotropic behavior, and the  $\text{FD}(\nu' = 4)$  state displays a more pronounced increase with energy. In analyzing this behavior in more detail, we observed that at  $3.5 \text{ kcal mol}^{-1}$ , while the  $\text{FD}(\nu' = 2)$  presents a sudden fall, the  $\text{FD}(\nu' = 4)$  presents a sudden rise, and the two effects compensate each other in the total function. Unfortunately, there are no experimental measurements for comparison, and at present we find no clear explanation for these effects.

Finally, it is interesting to compare the very different shapes of the excitation function found for the  $\text{F} + \text{CH}_4$  (ref 1) and  $\text{F} + \text{CD}_4$  reactions using the PES-2006 surface. While the former has an oscillating pattern associated with a quasi-trapped state, and reminiscent of a signature of a reactive resonance, which

**TABLE 4:  $\text{FD}(\nu')$  Vibrational Populations at a Collision Energy 5.4  $\text{kcal mol}^{-1}$ , with the  $\text{CD}_3$  Coproduct in its Ground State,  $\text{CD}_3(\nu = 0)$** 

reference	$\nu' = 0$	$\nu' = 1$	$\nu' = 2$	$\nu' = 3$	$\nu' = 4$	$\nu' = 5$
this work			0.07	0.62	0.31	
expt <sup>a</sup>			0.02	0.33	0.65	
PES-2005 <sup>b</sup>	0.06	0.40	0.44	0.10	0.02	
CABMFV <sup>c</sup>	0.01	0.02	0.10	0.24	0.38	0.22

<sup>a</sup> Reference 4. <sup>b</sup> LEPS-type surface from ref 3. <sup>c</sup> Interpolated ab initio surface at the MP-SAC2 level, from ref 25.

has been experimentally reported,<sup>9</sup> the latter has a smooth variation, indicative of a direct mechanism, again in agreement with experiment.<sup>4</sup> This satisfactory behavior of the PES-2006 surface for the two isotopic variants,  $\text{CH}_4$  and  $\text{CD}_4$ , reproducing the experimental observations, lends confidence to the surface.

**(C)  $\text{FD}(\nu', j')$  Product Rovibrational Distribution.** The QCT  $\text{FD}(\nu')$  vibrational distributions for the  $\text{CD}_3(\nu = 0)$  state using different surfaces are listed in Table 4 at a collision energy of  $5.4 \text{ kcal mol}^{-1}$ , together with the available experimental data for comparison.<sup>4</sup>

First, PES-2006 notably improves the results of our previous PES-2005 surface which gives colder vibrational distributions and of the interpolated ab initio surface of Castillo et al.<sup>25</sup> which shows isotropic behavior with hotter vibrational states,  $\text{FD}(\nu' = 5)$ . Second, our results agree qualitatively with experiment, although they are slightly colder by 1 unit of  $\nu$ . To analyze the possible reasons of this discrepancy, a more detailed analysis is necessary at this point. First, the difference can be due to deficiencies of the PES. However, in the previous study on the similar  $\text{F} + \text{CH}_4$  reaction,<sup>1</sup> we found that the  $\text{FH}(\nu')$  vibrational distribution peaks in  $\nu' = 2$  reproduce the experimental evidence. Second, the difference can be due to deficiencies of the QCT calculations. Zhou et al.<sup>7</sup> found experimentally a strong dependence of the FD vibrational branching ratio on the  $\text{CD}_3$  coproduct rotational states ( $N$ ). They reported that the distribution changes from  $\nu' = 4$  at low rotational states ( $N = 3$ ) to  $\nu' = 3$  at high rotational states ( $N = 9$ ), that is, the branching ratio  $\nu' = 4/\nu' = 3$  diminishes with the  $\text{CD}_3$  rotational excitation. In our previous work on the analogous  $\text{F} + \text{CH}_4$  reaction,<sup>1</sup> we found that the  $\text{FH}(\nu')$  rotational distributions are broader than experiment, which seems to be a general tendency of QCT calculations. In the present discussion, also it is necessary to take into account that the difference between  $N = 3$  and 9 is very small,  $1.07 \text{ kcal mol}^{-1}$ .<sup>26</sup> Because a more rigorous analysis is not possible with the QCT method because of its being unable of quantizing the  $\text{CD}_3$  rotational energy, we made an estimate of the effect of the  $\text{CD}_3(\nu' = 0)$  rotational excitation on the  $\text{FD}(\nu')$  vibrational distribution, considering the lowest (up to  $0.4 \text{ kcal mol}^{-1}$ ) and highest (from  $4.0 \text{ kcal mol}^{-1}$ ) rotational

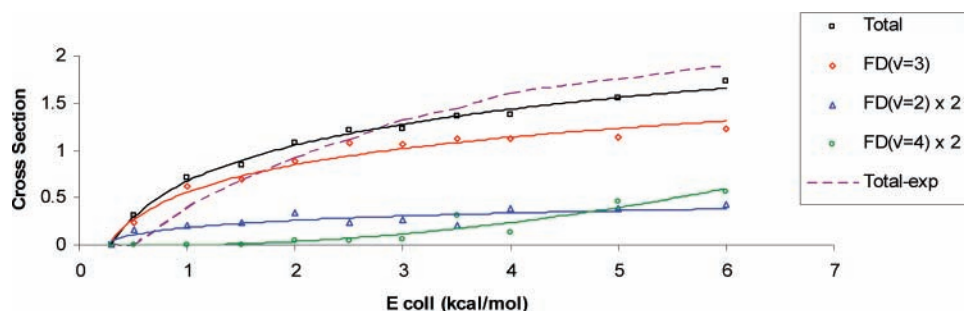


**Figure 1.** Excitation function (reaction cross section, in  $\text{\AA}^2$ , versus the collision energy, in  $\text{kcal mol}^{-1}$ ) for the  $\text{F} + \text{CD}_4 \rightarrow \text{FD}(\nu') + \text{CD}_3(\nu' = 0)$  reaction using the PES-2006 surface. The black line includes all  $\text{FD}(\nu')$  vibrational states. The red, blue, and green lines correspond to  $\text{FD}(\nu' = 3)$ ,  $\text{FD}(\nu' = 2)$ ,  $\text{FD}(\nu' = 4)$  levels, respectively. Note that the values for the  $\text{FD}(\nu' = 2)$  and  $\text{FD}(\nu' = 4)$  levels are multiplied by 2. Experimental values (dashed line) are read from Figure 4 of ref 5. The total distributions are normalized so that the area under the common range is the same.

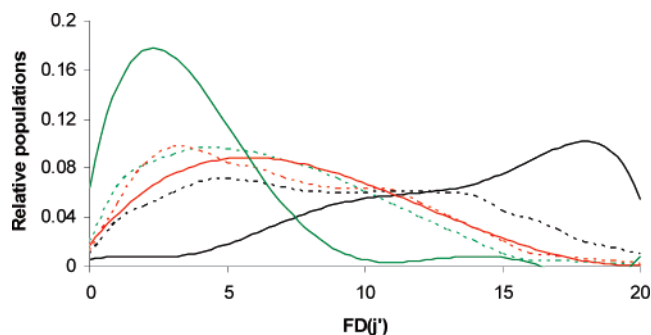


**Figure 2.** Rotational populations for  $F + CD_4 \rightarrow FD(v', j') + CD_3(v' = 0)$  reaction at a collision energy of  $5.4 \text{ kcal mol}^{-1}$ . The distributions are normalized so that the area under the common levels is the same. The black, red, and green lines correspond to  $FD(v' = 2, 3, \text{ and } 4)$ , respectively. Solid lines are from present work, and dashed lines are from ref 25.

energies of the  $CD_3$  coproduct. The rotational energy is obtained directly from the product energy partition in the reactive trajectories. For the former, the  $FD(v' = 1, 2, 3, 4)$  vibrational distributions are 0, 7, 64, and 29%, respectively, while for the latter they are 0, 28, 72, and 0%, respectively. Therefore, in both cases  $FD(v' = 3)$  is the most populated state, but the branching ratio  $v' = 4/v' = 3$  diminishes with the  $CD_3$  rotation, in agreement with experiment. In sum, the small differences found in the present work for the  $FD(v')$  vibrational distribution could be due to the QCT method's defective treatment of the rotational distributions.

Finally, this same analysis was performed at lower collision energy with similar results. Thus, at  $1.8 \text{ kcal mol}^{-1}$  collision energy we find the following  $FD(v' = 1, 2, 3, 4)$  vibrational distribution: 0, 12, 87, and 1%, respectively, and also for the  $CD_3$  coproduct in its ground state. Therefore, using PES-2006,  $FD(v' = 3)$  is the most populated state.

The QCT vibrationally resolved  $FD(v')$  rotational distributions for the  $CD_3(v = 0)$  state are plotted in Figure 2 at a collision energy of  $5.4 \text{ kcal mol}^{-1}$ . These distributions are broad and peak at  $j' = 18, 6, \text{ and } 2$  for  $FD(v' = 2, 3, 4)$ , respectively, that is, the rotational distributions are colder as the  $FD$  vibrational state increases. These broad rotational distributions are coherent with the discussion above about the role of the  $CD_3$  coproduct rotational distribution on the  $FD(v')$  vibrational branching ratio. Unfortunately, there is no experimental information for comparison, but these results qualitatively agree with those obtained by Castillo et al.<sup>25</sup> using a very different surface, with the most significant difference being for the  $FD(v' = 2)$  state. Those authors, however, reported a hotter rotational distribution when the  $FD(v')$  states pass from  $v' = 3$  to  $v' = 4$ .

**(D) Differential Cross Section.** The PES-2006  $FD$  product differential scattering dynamics for the  $CD_3(v' = 0)$  state at a  $5.4 \text{ kcal mol}^{-1}$  collision energy is plotted in Figure 3 together with the experimental data<sup>4</sup> and other QCT calculations on different surfaces, the interpolated *ab initio*<sup>25</sup> and our earlier PES-2005,<sup>3</sup> for comparison. First, the present results reproduce the steplike behavior found experimentally and agree reasonably well with experiment, where the forward shape dominates. Comparing these results with previous QCT calculations on different surfaces, one observes that the interpolated *ab initio* surface of Castillo et al.<sup>25</sup> gave predominantly backward scattering, and the PES-2005 gave sideways scattering, both far from experiment.

In analyzing this behavior with more detail, Figure 4 plots the QCT vibrationally state-resolved  $FD(v')$  scattering angular distributions (again, for the  $CD_3(v' = 0)$  state) at two collision

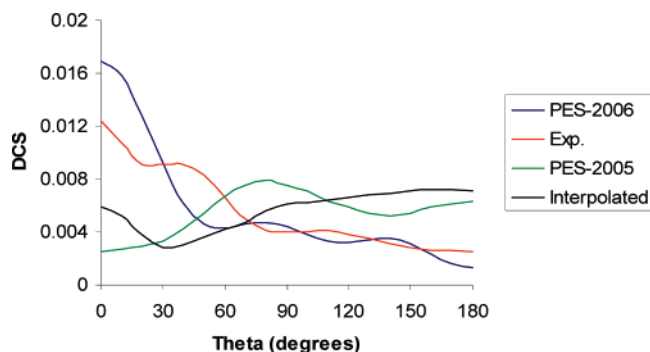


**Figure 3.** Product angular distribution for the  $F + CD_4 \rightarrow FD(v') + CD_3(v' = 0)$  reaction at a collision energy of  $5.4 \text{ kcal mol}^{-1}$  from different surfaces and experiment for comparison. The distributions are normalized so that the area under the common range is the same.

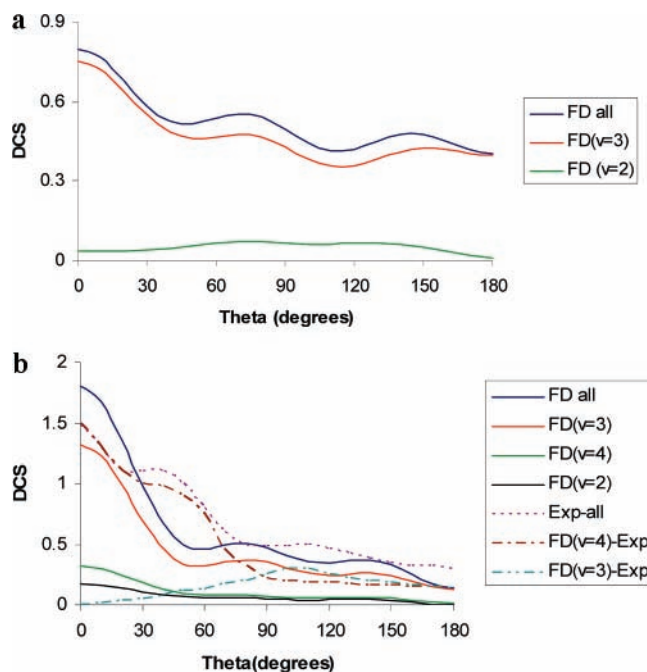


**Figure 4.** Product angular distribution for the  $F + CD_4 \rightarrow FD(v') + CD_3(v' = 0)$  reaction at collision energies of (a) 1.5 and (b)  $5.4 \text{ kcal mol}^{-1}$ , for different vibrational  $FD$  states. Panel b: Experimental values from ref 4 in dashed line.

energies, 1.5 and  $5.4 \text{ kcal mol}^{-1}$ . At the lower energy, the overall scattering function is fairly isotropic, with a clear tendency toward forward scattering. The shapes of the DCSs depend on the  $FD(v')$  states, with the  $FD(v' = 3)$  state dominating the overall DCS. At the higher collision energy,  $5.4 \text{ kcal mol}^{-1}$ , the overall scattering function is more forward. All the  $FD(v')$  state contributions are also forward, with the  $FD(v' = 3)$  state dominating the overall scattering function. In Figure 4b, the experimental data<sup>4</sup> are also included for comparison. The  $FD(v' = \text{all})$  distribution is well reproduced by our QCT calculations, as well as the scattering distribution for the most populated vibrational state,  $v' = 4$  and 3, for experiment and QCT calculations, respectively.

To shed more light on this situation, we analyzed the evolution of the angular distribution as a function of the collision energy for the most populated  $FD(v' = 3)$  state. The three-dimensional  $DCS-E_{\text{coll}}-\theta$  representation is plotted in Figure 5. One observes a mild change of DCS with collision energy, from backward scattering at low energies to forward scattering at high energies, which seems to indicate a direct mechanism for the  $F + CD_4$  reaction. This signature first reproduces the

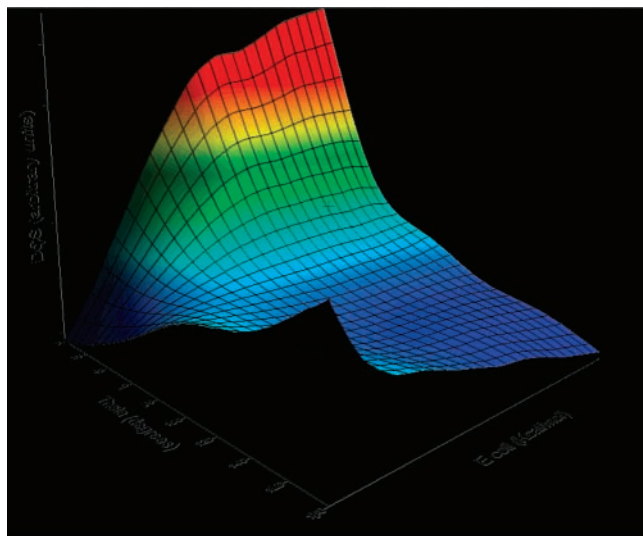


**Figure 5.** Three-dimensional representation of the evolution of the differential cross section as a function of the collision energy in the range 0.3–6.0 kcal mol<sup>-1</sup>.

experimental information<sup>6</sup> that the DCS becomes increasingly forward as the collision energy increases and second is remarkably different from that obtained for the analogous F + CH<sub>4</sub> reaction,<sup>1</sup> which seems to indicate that there are different mechanisms for the two isotopes.

#### IV. Conclusions

In this work, on an analytical potential energy surface (PES-2006) recently developed by our group for the F + CD<sub>4</sub> → FD + CD<sub>3</sub> gas-phase abstraction reaction, an extensive state-to-state dynamics study was performed using quasi-classical trajectory (QCT) calculations. In this QCT study, the zero-point energy problem to avoid leakage along the trajectories was explicitly considered, and the collision energies ranged from 0.3 to 6.0 kcal mol<sup>-1</sup>.

Most of the available energy appears as FD(*v'*) vibrational energy, with the FD(*v'*) product found to be vibrationally hot although less excited than experiment by one quantum, and rotationally cold. Moreover, we found a normal negative correlation between product vibrational and rotational excitations. The CD<sub>3</sub> coproduct presented a small internal energy, in agreement with experiment.

The excitation function showed standard behavior, rising from the threshold and then leveling off at higher collision energies, in accordance with experiment. The product angular scattering distributions at different collision energies reproduced the experimental measurements. The forward scattering predominated at all energies, increasing with increasing energy.

The dynamics results obtained with the analytical PES-2006 surface remarkably improved those of earlier surfaces, the interpolated ab initio of Castillo et al.<sup>25</sup> and our previous PES-2005.<sup>3</sup>

Finally, the comparison of the dynamics results for the title reaction, F + CD<sub>4</sub>, with those for the analogous F + CH<sub>4</sub> reaction recently reported by our group<sup>1</sup> showed different behavior of the excitation function and of the evolution of the differential cross section with collision energy. These different patterns seem to indicate that the two reactions follow different mechanisms.

**Acknowledgment.** This work was partially supported by the Junta de Extremadura, Spain (Project No. 2PR04A001).

#### References and Notes

- (1) Espinosa-García, J.; Bravo, J. L.; Rangel, C. *J. Phys. Chem. A* **2007**, *111*, 2761.
- (2) Corchado, J. C.; Espinosa-García, J. *J. Chem. Phys.* **1996**, *105*, 3152.
- (3) Rangel, C.; Navarrete, M.; Espinosa-García, J. *J. Phys. Chem. A* **2005**, *109*, 1441.
- (4) Lin, J. J.; Zhou, J.; Shiu, W.; Liu, K. *Science* **2003**, *300*, 966.
- (5) Zhou, J.; Lin, J. J.; Shiu, W.; Pu, S.-C.; Liu, K. *J. Chem. Phys.* **2003**, *119*, 2538.
- (6) Zhou, J.; Lin, J. J.; Shiu, W.; Liu, K. *J. Chem. Phys.* **2003**, *119*, 4997.
- (7) Zhou, J.; Shiu, W.; Lin, J. J.; Liu, K. *J. Chem. Phys.* **2004**, *120*, 5863.
- (8) (a) Shimonuchi, T. *Tables of Molecular Vibrational Frequencies Consolidated Volume I*; National Bureau of Standards, 1972; pp 1–160. (b) Brum, J. L.; Johnson, R. D.; Hudgens, J. W. *J. Chem. Phys.* **1993**, *98*, 3732. (c) Spanbauer, R. N.; Rao, K. N. *J. Mol. Spectrosc.* **1965**, *16*, 100. (d) Chase, M. W.; Davis, C. A.; Downey, J. R.; Frurip, D. J.; McDonald, R. A.; Syverud, A. N. JANAF Thermochemical tables. *J. Phys. Chem. Ref. Data Suppl.* **1985**, *14*.
- (9) Shiu, W.; Lin, J. J.; Liu, K. *Phys. Rev. Lett.* **2004**, *92*, 103201.
- (10) Porter, R. N.; Raff, L. M. In *Dynamics of Molecular Collisions*; Miller, W. H., Ed.; Plenum Press: New York, 1976; Part B.
- (11) Truhlar, D. G.; Muckerman, J. T. In *Atom-molecules Collision Theory*; Bernstein, R. B., Ed.; Plenum Press: New York, 1979.
- (12) Raff, L. M.; Thompson, D. L. In *Theory of Chemical Reaction Dynamics*; Baer, M., Ed.; CRC Press: Boca Raton, FL, 1985; Vol. 3.
- (13) Hase, W. L.; Duchovic, R. J.; Hu, X.; Komornicki, A.; Lim, K. F.; Lu, D.-h.; Peshlherbe, G. H.; Swamy, K. N.; Van de Linde, S. R.; Varandas, A. J. C.; Wang, H.; Wolf, R. J. VENUS96: A General Chemical Dynamics Computer Program. *QCPE Bull.* **1996**, *16*, 43.
- (14) Rangel, C.; Corchado, J. C.; Espinosa-García, J. *J. Phys. Chem. A* **2006**, *110*, 10375.
- (15) Bowman, J. M.; Kuppermann, A. *J. Chem. Phys.* **1973**, *59*, 6524.
- (16) Truhlar, D. G. *J. Phys. Chem.* **1979**, *83*, 18.
- (17) Schatz, G. C. *J. Chem. Phys.* **1983**, *79*, 5386.
- (18) Lu, D.-h.; Hase, W. L. *J. Chem. Phys.* **1988**, *89*, 6723.
- (19) Varandas, A. J. C. *Chem. Phys. Lett.* **1994**, *225*, 18.
- (20) Ben-Nun, M.; Levine, R. D. *J. Chem. Phys.* **1996**, *105*, 8136.
- (21) McCormack, D. A.; Lim, K. F. *Phys. Chem. Chem. Phys.* **1999**, *1*, 1.
- (22) Stock, G.; Müller, U. *J. Chem. Phys.* **1999**, *111*, 65.
- (23) Marques, J. M. C.; Martínez-Núñez, E.; Fernández-Ramos, A.; Vázquez, S. *J. Phys. Chem.* **2005**, *109*, 5415.
- (24) Duchovic, R. J.; Parker, M. A. *J. Phys. Chem.* **2005**, *109*, 5883.
- (25) Castillo, J. F.; Aoz, F. J.; Bañares, L.; Martínez-Núñez, A.; Fernández-Ramos, A.; Vázquez, S. *J. Phys. Chem. A* **2005**, *109*, 8459.
- (26) Frye, J. M.; Sears, T. J.; Leitner, D. *J. Chem. Phys.* **1988**, *88*, 5300.